Nuclear Physics B105 (1976) 253–271
North-Holland Publishing Company

ELECTROPRODUCTION OF NEUTRAL PIONS IN THE RESONANCE REGION

J.-C. ALDER*, F.W. BRASSE, W. FEHRENBACH**, J. GAYLER, S.P. GOEL‡, R. HAIDAN, V. KORBEL‡‡, J. MAY‡‡ M. MERKWITZ and A. NURIMBA
Deutsches Elektronen-Synchrotron DESY, Hamburg, Germany

Received 31 October 1975
(Revised 1 December 1975)

Results on the reaction $ep \to e'p\pi^0$ are presented in the mass range $1.355 \leq W \leq 1.745$ GeV at $q^2 \approx 1$ GeV^2 and in the range $1.415 \leq W \leq 1.595$ GeV at $q^2 \approx 0.6$ GeV^2. From the angular distribution of the π^0 meson the polarization terms $\sigma_U + \epsilon\sigma_L$, σ_P and σ_I have been determined in a range of production angles from $\theta^* \gtrsim 50°$ up to $\theta^* = 180°$. Results on the total $\gamma_V p \to \pi^0 p$ cross section are given.

1. Introduction

We have reported on an experiment on electroproduction of η mesons [1] and π^+ mesons [2] in the resonance region. Now we report on the data of the reaction $ep \to ep\pi^0$ taken at the same experiment.

There exist data on π^0 production from Daresbury at $q^2 \approx 0.4$ and 0.6 GeV^2 [3] in the second resonance region and some data from DESY [4] in the third resonance region and above in a limited angular range. The present experiment covers the second resonance region ($q^2 \approx 0.6$, 1 GeV^2) and the third resonance region ($q^2 \approx 1$ GeV^2). The angular distributions obtained have been analysed in terms of the polarization terms $\sigma_U + \epsilon\sigma_L$, σ_P and σ_I.

In a recent multipole analysis of the existent data on pion production Devenish and Lyth [5] described the resonance region in terms of 11 resonances. These authors also used a preliminary subset of the present data. It is the purpose of the present experiment to allow for a determination of the couplings of the relevant resonances in the covered kinematic range.

Present addresses:
* Université de Lausanne.
** Babcock-Brown-Boveri, Mannheim.
‡ On leave from Kurukshetra University, Kurukshetra, India.
‡‡ CERN, Geneva.

2. Notation

We express the cross section in terms of the virtual photon absorption cross section $d\sigma/d\Omega^*_{\pi 0}$ in the c.m.s. of the final hadrons which is related to the differential coincidence cross section $d^5\sigma/dE'\, d\Omega_e\, d\Omega^*_{\pi 0}$ by the virtual photon flux factor Γ_t (defined as usually [6]):

$$\frac{d^5\sigma}{dE'\, d\Omega_e d\Omega^*_{\pi 0}} = \Gamma_t \frac{d\sigma}{d\Omega^*_{\pi 0}} \,. \tag{1}$$

The polar and aximuthal production angles (fig. 1) in the c.m.s. are denoted by θ^* and ϕ. The ϕ dependence of the angular distribution in the c.m.s. can be written explicitly as [7]:

$$\frac{d\sigma}{d\Omega^*_{\pi 0}} = \sigma_U + \epsilon\sigma_L + \epsilon \cos 2\phi\, \sigma_P + \sqrt{2\epsilon(\epsilon+1)} \cos\phi\, \sigma_I \,. \tag{2}$$

The parameter ϵ describes the polarization of the virtual photon (e.g. ref. [6]). The cross sections σ_U, σ_L, σ_P and σ_I are functions of the invariant mass W of the final $p\pi^0$ system, the momentum transfer q^2, and the angle θ^*.

The terms σ_U and σ_L are the cross sections of unpolarized transverse and longitudinal virtual photons. They can only be separated by changing the polarization ϵ, not done in this experiment. σ_P takes account of the transverse polarization of the virtual photon and σ_I is a transverse-longitudinal interference term. A study of the ϕ dependence for fixed θ^* allows to separate the 3 terms $\sigma_U + \epsilon\sigma_L$, σ_P and σ_I.

If in addition to one photon exchange we assume that only S, P and D waves contribute, with total angular momentum $j \leqslant \frac{3}{2}$, we can express the cross section in

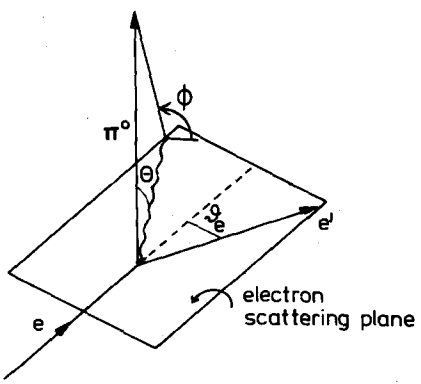

Fig. 1. Definition of the angles.

terms of angular coefficients (cf. e.g. ref. [3]):

$$\sigma_U + \epsilon\sigma_L = \bar{A}_0 + \bar{A}_1 \cos\theta^* + \bar{A}_2 \cos^2\theta^* + \bar{A}_3 \cos^3\theta^* ,$$

$$\sigma_P = (C_0 + C_1 \cos\theta^*) \sin^2\theta^* . \tag{3}$$

$$\sigma_I = (D_0 + D_1 \cos\theta^* + D_2 \cos^2\theta^*) \sin\theta^* .$$

If we allow for F waves with $j = \frac{5}{2}$ the following 3 terms

$$\bar{A}_4 \cos^4\theta^*, \quad C_2 \cos^2\theta^* \sin^2\theta^*, \quad D_3 \cos^3\theta^* \sin\theta^*$$

have to be added. The total virtual photoproduction cross section is then given by:

$$\sigma_{tot} = 4\pi (\bar{A}_0 + \tfrac{1}{3}\bar{A}_2 + \tfrac{1}{5}\bar{A}_4) . \tag{4}$$

3. Apparatus

The experimental set-up is described in more detail in ref. [1]. Only a short description is repeated here. The measurements are done in an external e^- beam of DESY. The primary beam hits a 12 cm liquid hydrogen target. The intensity is controlled by a secondary emission monitor, which was compared many times during the experiment to a Faraday cup. The scattered electron is detected in a double focussing vertically bending spectrometer. It is identified by a threshold Čerenkov- and a sandwich shower counter.

The secondary proton is detected in coincidence with the scattered e^- in a non focussing spectrometer consisting of a vertically bending magnet, a system of proportional chambers mounted at the magnet exit, and a scintillator hodoscope.

4. Data analysis

The secondary protons are distinguished from π^+ mesons by time of flight [1]. Some pion background in the remaining proton sample was rejected by requirement of sufficient pulse height of scintillator signals.

The reaction $ep \to ep\pi^0$ was determined by the requirement of appropriate missing mass, computed from the detected electron and proton. An example of a missing mass squared distribution is given in fig. 2. Events in the range of missing mass squared from -0.02 to 0.07 GeV^2 have been used to calculate the cross sections of the reaction $ep \to ep\pi^0$. The chosen bins were $\Delta W = 30$ MeV, $\Delta\cos\theta^* = 0.1$, $\Delta\phi = 20°$. The acceptance of the electron spectrometer determines the bin size in q^2 to $\Delta q^2 \approx 0.07$ and 0.1 GeV^2 at $q^2 = 0.6$ and 1 GeV^2 respectively.

Acceptances and various corrections have been calculated by a Monte-Carlo simulation of the experiment. Radiative corrections have been incorporated into the

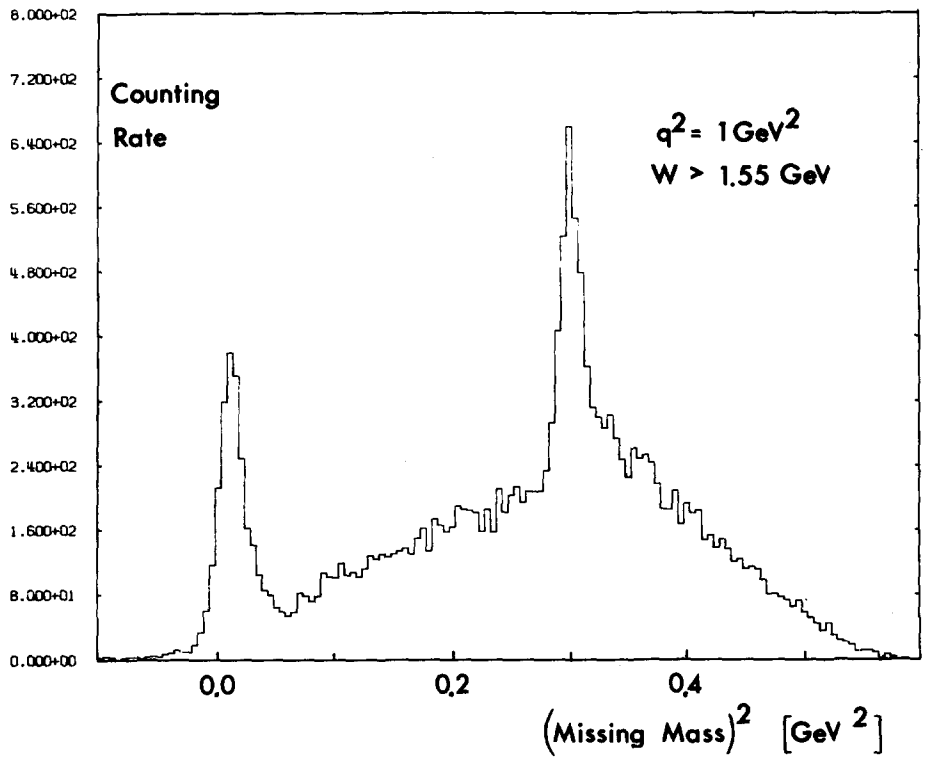

Fig. 2. Example of a distribution of missing mass squared computed from the detected protons in coincidence with electrons.

simulation including internal and external radiation. In this simulation the radiation of the electron has been taken into account in the peaking approximation according to the formulas of ref. [8]. Some multipion background has also been included into the simulation, leading to correction smaller than 3%.

The cross sections are corrected for empty target rate (≈0.5%). nuclear absorption (≈1.5%), dead time losses, inefficiencies, multi-track events and random background.

5. Results

All data have been taken with the central electron spectrometer angle set to 15°. The polarization ϵ was always close to 0.9 (see table 1). The errors given in the figures are statistical only. We estimate an overall systematic error of 6%.

Table 1
Angular distribution of the reaction $\gamma_V p \to \pi^0 p$. The errors do not contain an overall systematic error of 6%.

$\cos\theta^*$	$\sigma_U + \epsilon\sigma_L$	σ_P (μb/sr)	σ_I
	W = 1.355 GeV	ϵ = 0.93	q^2 = 1.05 GeV^2
-0.985	0.88 +- 0.11		
-0.750	1.16 +- 0.09	-0.20 +- 0.13	-0.02 +- 0.06
-0.650	1.35 +- 0.09	-0.40 +- 0.16	-0.06 +- 0.07
-0.550	1.73 +- 0.11	-0.70 +- 0.19	-0.21 +- 0.08
-0.450	1.88 +- 0.12	-0.62 +- 0.22	0.09 +- 0.09
-0.350	2.13 +- 0.15	-0.90 +- 0.30	0.03 +- 0.13
-0.250	2.62 +- 0.21	-0.31 +- 0.41	-0.21 +- 0.17
-0.150	2.67 +- 0.28	-1.13 +- 0.57	-0.08 +- 0.22
-0.050	2.50 +- 0.21	-0.84 +- 0.38	-0.06 +- 0.16
0.050	2.25 +- 0.17	-0.90 +- 0.33	-0.03 +- 0.15
0.150	2.60 +- 0.19	-1.18 +- 0.34	-0.04 +- 0.18
0.250	2.02 +- 0.17	-1.30 +- 0.33	-0.13 +- 0.17
0.350	2.48 +- 0.21	-0.99 +- 0.37	-0.11 +- 0.19
0.450	1.93 +- 0.18	-1.28 +- 0.33	-0.15 +- 0.18
0.550	1.63 +- 0.20	-1.10 +- 0.31	-0.23 +- 0.19
0.650	1.58 +- 0.29	-0.18 +- 0.35	-0.22 +- 0.25
	W = 1.385 GeV	ϵ = 0.93	q^2 = 1.04 GeV^2
-0.985	0.50 +- 0.06		
-0.850	0.56 +- 0.22	-0.25 +- 0.24	-0.22 +- 0.19
-0.750	0.84 +- 0.06	-0.17 +- 0.08	-0.12 +- 0.05
-0.650	1.02 +- 0.06	-0.14 +- 0.10	-0.14 +- 0.05
-0.550	1.49 +- 0.09	-0.40 +- 0.16	-0.12 +- 0.08
-0.450	1.29 +- 0.09	-0.46 +- 0.19	0.05 +- 0.09
-0.350	1.50 +- 0.13	-0.28 +- 0.25	-0.13 +- 0.13
-0.250	1.94 +- 0.12	-0.57 +- 0.22	-0.04 +- 0.10
-0.150	2.05 +- 0.12	-0.66 +- 0.21	0.10 +- 0.09
-0.050	1.93 +- 0.12	-1.03 +- 0.22	-0.01 +- 0.11
0.050	1.89 +- 0.12	-0.55 +- 0.22	0.08 +- 0.11
0.150	1.66 +- 0.12	-1.03 +- 0.23	-0.05 +- 0.11
0.250	1.77 +- 0.14	-0.67 +- 0.24	0.02 +- 0.13
0.350	1.71 +- 0.13	-0.81 +- 0.26	-0.07 +- 0.13
0.450	1.54 +- 0.13	-0.35 +- 0.24	-0.08 +- 0.12
0.550	1.61 +- 0.16	-0.53 +- 0.25	0.01 +- 0.14
0.650	0.92 +- 0.17	-0.59 +- 0.23	-0.29 +- 0.15
	W = 1.415 GeV	ϵ = 0.93	q^2 = 1.03 GeV^2
-0.985	0.50 +- 0.06		
-0.935	0.62 +- 0.10	0.20 +- 0.13	-0.05 +- 0.08
-0.850	0.44 +- 0.13	-0.05 +- 0.17	-0.16 +- 0.11
-0.750	0.67 +- 0.24	-0.09 +- 0.26	-0.10 +- 0.20
-0.650	0.85 +- 0.06	-0.14 +- 0.11	-0.17 +- 0.06
-0.550	1.26 +- 0.09	-0.34 +- 0.17	-0.08 +- 0.10
-0.450	1.31 +- 0.09	-0.18 +- 0.15	-0.04 +- 0.08
-0.350	1.58 +- 0.09	-0.68 +- 0.14	0.03 +- 0.06
-0.250	1.65 +- 0.08	-0.53 +- 0.14	-0.14 +- 0.06
-0.150	1.68 +- 0.09	-0.33 +- 0.15	-0.06 +- 0.07
-0.050	1.57 +- 0.09	-0.33 +- 0.16	0.01 +- 0.08
0.050	1.59 +- 0.10	-0.35 +- 0.18	0.04 +- 0.09
0.150	1.58 +- 0.11	-0.09 +- 0.20	0.08 +- 0.10
0.250	1.68 +- 0.13	-0.24 +- 0.24	0.19 +- 0.11
0.350	1.88 +- 0.15	0.00 +- 0.26	0.16 +- 0.12
0.450	1.54 +- 0.14	0.29 +- 0.23	0.18 +- 0.12
0.550	1.11 +- 0.15	-0.08 +- 0.25	-0.28 +- 0.11
0.650	1.15 +- 0.43	0.04 +- 0.44	0.23 +- 0.35

Table 1 (continued)

$\cos\theta^*$	$\sigma_U + \epsilon\sigma_L$	σ_P	σ_I
		(μb/sr)	
	W = 1.445 GeV	ϵ = 0.92	q^2 = 1.02 GeV^2
-0.985	0.22 +- 0.04		
-0.935	0.64 +- 0.13	0.24 +- 0.18	0.02 +- 0.10
-0.850	0.47 +- 0.11	-0.02 +- 0.16	-0.18 +- 0.10
-0.650	0.97 +- 0.09	-0.01 +- 0.14	-0.21 +- 0.09
-0.550	1.05 +- 0.09	-0.14 +- 0.14	-0.23 +- 0.09
-0.450	1.35 +- 0.08	-0.30 +- 0.11	-0.19 +- 0.05
-0.350	1.50 +- 0.08	-0.30 +- 0.11	-0.15 +- 0.05
-0.250	1.47 +- 0.08	-0.29 +- 0.12	-0.06 +- 0.05
-0.150	1.77 +- 0.09	-0.20 +- 0.15	-0.09 +- 0.07
-0.050	1.67 +- 0.09	-0.46 +- 0.17	0.00 +- 0.07
0.050	1.49 +- 0.10	-0.12 +- 0.18	-0.01 +- 0.08
0.150	1.59 +- 0.13	-0.11 +- 0.23	0.08 +- 0.10
0.250	1.48 +- 0.15	-0.32 +- 0.26	-0.06 +- 0.11
0.350	1.70 +- 0.18	0.52 +- 0.28	-0.00 +- 0.12
0.450	1.59 +- 0.18	0.53 +- 0.28	-0.16 +- 0.12
	W = 1.475 GeV	ϵ = 0.92	q^2 = 1.01 GeV^2
-0.985	0.34 +- 0.06		
-0.935	0.45 +- 0.06	0.12 +- 0.10	0.04 +- 0.05
-0.850	0.48 +- 0.07	-0.09 +- 0.11	-0.18 +- 0.05
-0.750	1.02 +- 0.23	0.30 +- 0.33	-0.07 +- 0.11
-0.650	1.02 +- 0.11	0.09 +- 0.14	-0.24 +- 0.10
-0.550	1.24 +- 0.07	-0.13 +- 0.09	-0.34 +- 0.05
-0.450	1.30 +- 0.07	-0.16 +- 0.10	-0.22 +- 0.04
-0.350	1.55 +- 0.07	-0.16 +- 0.11	-0.14 +- 0.05
-0.250	1.91 +- 0.09	-0.53 +- 0.14	-0.22 +- 0.06
-0.150	1.70 +- 0.09	-0.55 +- 0.17	-0.06 +- 0.07
-0.050	1.78 +- 0.11	-0.69 +- 0.21	0.04 +- 0.08
0.050	1.79 +- 0.15	-0.85 +- 0.28	-0.07 +- 0.12
0.150	2.06 +- 0.20	0.03 +- 0.32	-0.29 +- 0.15
0.250	1.82 +- 0.23	-0.12 +- 0.37	-0.20 +- 0.16
	W = 1.505 GeV	ϵ = 0.92	q^2 = 0.99 GeV^2
-0.985	0.30 +- 0.06		
-0.935	0.54 +- 0.07	0.13 +- 0.13	-0.12 +- 0.06
-0.850	0.70 +- 0.08	-0.03 +- 0.14	-0.27 +- 0.05
-0.650	1.08 +- 0.08	-0.06 +- 0.10	-0.27 +- 0.07
-0.550	1.23 +- 0.07	-0.06 +- 0.09	-0.20 +- 0.05
-0.450	1.53 +- 0.07	-0.14 +- 0.10	-0.18 +- 0.05
-0.350	1.76 +- 0.08	-0.58 +- 0.14	-0.15 +- 0.06
-0.250	1.95 +- 0.10	0.02 +- 0.16	-0.32 +- 0.08
-0.150	2.08 +- 0.12	-0.45 +- 0.21	-0.28 +- 0.10
-0.050	1.99 +- 0.17	-0.43 +- 0.27	-0.32 +- 0.14
0.050	2.11 +- 0.22	-0.12 +- 0.32	-0.04 +- 0.17
0.150	2.26 +- 0.35	0.12 +- 0.47	-0.25 +- 0.25
	W = 1.535 GeV	ϵ = 0.91	q^2 = 0.98 GeV^2
-0.985	0.43 +- 0.08		
-0.935	0.55 +- 0.06	-0.02 +- 0.11	-0.06 +- 0.05
-0.850	0.59 +- 0.08	-0.12 +- 0.12	-0.06 +- 0.07
-0.750	0.74 +- 0.07	-0.08 +- 0.12	-0.18 +- 0.06
-0.650	0.87 +- 0.10	-0.26 +- 0.18	-0.23 +- 0.11
-0.550	0.91 +- 0.06	-0.00 +- 0.08	-0.16 +- 0.04
-0.450	1.26 +- 0.07	-0.12 +- 0.10	-0.14 +- 0.05
-0.350	1.44 +- 0.08	-0.10 +- 0.12	-0.22 +- 0.07
-0.250	1.41 +- 0.10	-0.63 +- 0.16	-0.01 +- 0.09
-0.150	1.68 +- 0.15	-0.30 +- 0.20	-0.30 +- 0.13
-0.050	1.85 +- 0.25	-0.64 +- 0.32	-0.13 +- 0.22
0.050	2.05 +- 0.44	-0.09 +- 0.51	-0.21 +- 0.35

Table 1 (continued)

$\cos\theta^*$	$\sigma_U + \epsilon\sigma_L$	σ_P	σ_I
		(μb/sr)	
	W = 1.565 GeV	ϵ = 0.91	q^2 = 0.97 GeV^2
-0.985	0.23 +- 0.04		
-0.935	0.46 +- 0.03	-0.03 +- 0.05	-0.04 +- 0.02
-0.850	0.59 +- 0.05	-0.13 +- 0.07	-0.06 +- 0.04
-0.750	0.57 +- 0.03	0.00 +- 0.06	-0.04 +- 0.03
-0.650	0.76 +- 0.05	-0.05 +- 0.10	-0.05 +- 0.05
-0.550	0.83 +- 0.04	-0.04 +- 0.06	-0.09 +- 0.03
-0.450	0.80 +- 0.04	0.04 +- 0.06	-0.05 +- 0.03
-0.350	1.14 +- 0.06	-0.07 +- 0.09	-0.10 +- 0.05
-0.250	1.31 +- 0.08	-0.14 +- 0.12	-0.13 +- 0.08
-0.150	1.41 +- 0.11	-0.23 +- 0.15	-0.10 +- 0.10
-0.050	1.33 +- 0.21	-0.33 +- 0.24	0.05 +- 0.18
	W = 1.595 GeV	ϵ = 0.90	q^2 = 0.95 GeV^2
-0.985	0.25 +- 0.04		
-0.935	0.41 +- 0.03	-0.10 +- 0.05	0.02 +- 0.02
-0.850	0.56 +- 0.05	-0.05 +- 0.08	-0.03 +- 0.05
-0.750	0.56 +- 0.03	-0.02 +- 0.05	-0.01 +- 0.02
-0.650	0.62 +- 0.04	0.14 +- 0.08	0.05 +- 0.04
-0.550	0.68 +- 0.04	-0.03 +- 0.05	-0.05 +- 0.03
-0.450	0.68 +- 0.04	-0.03 +- 0.06	-0.03 +- 0.04
-0.350	0.86 +- 0.06	-0.05 +- 0.08	-0.04 +- 0.05
-0.250	0.94 +- 0.08	0.03 +- 0.10	-0.11 +- 0.07
-0.150	1.10 +- 0.13	-0.07 +- 0.15	-0.09 +- 0.12
-0.050	0.95 +- 0.19	-0.46 +- 0.22	0.06 +- 0.16
	W = 1.625 GeV	ϵ = 0.90	q^2 = 0.94 GeV^2
-0.985	0.30 +- 0.04		
-0.935	0.45 +- 0.04	-0.04 +- 0.06	0.01 +- 0.03
-0.850	0.51 +- 0.03	-0.09 +- 0.04	0.07 +- 0.02
-0.750	0.52 +- 0.03	-0.07 +- 0.05	0.06 +- 0.02
-0.650	0.54 +- 0.03	-0.05 +- 0.06	0.00 +- 0.03
-0.550	0.52 +- 0.04	-0.03 +- 0.06	-0.04 +- 0.03
-0.450	0.66 +- 0.05	0.12 +- 0.07	-0.07 +- 0.04
-0.350	0.77 +- 0.06	-0.03 +- 0.08	-0.08 +- 0.06
-0.250	0.85 +- 0.09	-0.05 +- 0.11	-0.02 +- 0.09
-0.150	0.78 +- 0.14	-0.27 +- 0.15	0.05 +- 0.12
-0.050	0.81 +- 0.34	-0.30 +- 0.33	0.01 +- 0.29
	W = 1.655 GeV	ϵ = 0.90	q^2 = 0.93 GeV^2
-0.985	0.44 +- 0.04		
-0.935	0.58 +- 0.07	-0.19 +- 0.11	0.07 +- 0.07
-0.850	0.63 +- 0.03	-0.27 +- 0.04	0.12 +- 0.02
-0.750	0.51 +- 0.03	-0.05 +- 0.04	0.09 +- 0.02
-0.650	0.58 +- 0.03	0.08 +- 0.07	-0.04 +- 0.03
-0.550	0.60 +- 0.06	-0.03 +- 0.10	-0.00 +- 0.04
-0.450	0.62 +- 0.05	0.02 +- 0.07	-0.05 +- 0.05
-0.350	0.78 +- 0.08	0.09 +- 0.10	-0.12 +- 0.08
-0.250	0.67 +- 0.13	-0.24 +- 0.13	0.03 +- 0.12
-0.150	1.02 +- 0.32	0.01 +- 0.27	-0.19 +- 0.28

Table 1 (continued)

$\cos\theta^*$	$\sigma_U + \epsilon\sigma_L$	σ_P	σ_I
		(μb/sr)	
	W = 1.685 GeV	ϵ = 0.89	q^2 = 0.91 GeV^2
-0.985	0.80 +- 0.06		
-0.935	0.53 +- 0.17	-0.26 +- 0.23	0.32 +- 0.12
-0.850	0.54 +- 0.03	-0.15 +- 0.04	0.15 +- 0.02
-0.750	0.47 +- 0.03	-0.08 +- 0.04	0.11 +- 0.02
-0.650	0.51 +- 0.03	-0.11 +- 0.07	0.04 +- 0.03
-0.550	0.49 +- 0.06	-0.10 +- 0.11	-0.03 +- 0.04
-0.450	0.63 +- 0.07	0.02 +- 0.08	-0.10 +- 0.06
-0.350	0.65 +- 0.11	0.01 +- 0.10	-0.07 +- 0.10
-0.250	1.29 +- 0.30	0.24 +- 0.24	-0.56 +- 0.26
-0.150	1.17 +- 0.37	0.18 +- 0.28	-0.48 +- 0.31
	W = 1.715 GeV	ϵ = 0.88	q^2 = 0.90 GeV^2
-0.985	0.65 +- 0.06		
-0.935	0.42 +- 0.04	-0.13 +- 0.07	0.08 +- 0.04
-0.850	0.34 +- 0.02	-0.05 +- 0.04	0.11 +- 0.02
-0.750	0.33 +- 0.02	-0.08 +- 0.04	0.07 +- 0.02
-0.650	0.34 +- 0.03	-0.10 +- 0.06	0.02 +- 0.03
-0.550	0.42 +- 0.05	0.04 +- 0.08	-0.05 +- 0.04
-0.450	0.45 +- 0.07	0.04 +- 0.08	-0.12 +- 0.06
-0.350	0.46 +- 0.10	0.02 +- 0.09	-0.11 +- 0.09
-0.250	0.55 +- 0.29	-0.01 +- 0.22	-0.09 +- 0.25
	W = 1.745 GeV	ϵ = 0.88	q^2 = 0.88 GeV^2
-0.985	0.58 +- 0.07		
-0.935	0.34 +- 0.04	-0.11 +- 0.06	0.01 +- 0.03
-0.850	0.20 +- 0.02	-0.07 +- 0.03	0.02 +- 0.01
-0.750	0.24 +- 0.02	-0.06 +- 0.05	0.01 +- 0.02
-0.650	0.20 +- 0.03	0.01 +- 0.05	-0.01 +- 0.03
-0.550	0.30 +- 0.06	0.09 +- 0.09	-0.06 +- 0.05
	W = 1.415 GeV	ϵ = 0.92	q^2 = 0.63 GeV^2
-0.985	0.73 +- 0.14		
-0.750	1.22 +- 0.15	-0.57 +- 0.23	-0.11 +- 0.13
-0.550	1.88 +- 0.17	-0.77 +- 0.24	-0.22 +- 0.10
-0.450	2.41 +- 0.19	-0.91 +- 0.27	-0.13 +- 0.10
-0.350	2.48 +- 0.20	-0.86 +- 0.36	-0.20 +- 0.13
-0.250	3.14 +- 0.24	-1.03 +- 0.53	-0.20 +- 0.18
-0.150	2.88 +- 0.25	-2.14 +- 0.74	-0.40 +- 0.21
-0.050	2.61 +- 0.34	-1.53 +- 0.84	-0.00 +- 0.26
0.050	2.14 +- 0.39	-2.73 +- 1.07	-0.47 +- 0.30
	W = 1.445 GeV	ϵ = 0.92	q^2 = 0.62 GeV^2
-0.985	0.53 +- 0.08		
-0.935	0.47 +- 0.07	0.06 +- 0.13	-0.22 +- 0.06
-0.850	0.90 +- 0.20	0.04 +- 0.25	-0.16 +- 0.17
-0.650	1.32 +- 0.08	0.01 +- 0.12	-0.33 +- 0.06
-0.550	1.57 +- 0.09	-0.53 +- 0.13	-0.21 +- 0.04
-0.450	1.84 +- 0.09	-0.39 +- 0.15	-0.22 +- 0.05
-0.350	2.11 +- 0.10	-0.71 +- 0.20	-0.17 +- 0.06
-0.250	2.46 +- 0.13	-0.45 +- 0.33	-0.11 +- 0.10
-0.150	2.23 +- 0.15	-0.43 +- 0.36	-0.08 +- 0.11
-0.050	2.39 +- 0.22	-0.38 +- 0.47	0.04 +- 0.16

Table 1 (continued)

$\cos\theta^*$	$\sigma_U + \epsilon\sigma_L$	σ_T (μb/sr)	σ_I
	W = 1.475 GeV	ϵ = 0.91	q^2 = 0.61 GeV^2
-0.985	0.46 +- 0.07		
-0.935	0.52 +- 0.16	-0.00 +- 0.23	-0.23 +- 0.14
-0.850	0.83 +- 0.13	0.11 +- 0.20	-0.12 +- 0.08
-0.750	1.43 +- 0.24	0.49 +- 0.30	0.00 +- 0.20
-0.650	1.64 +- 0.08	-0.13 +- 0.11	-0.49 +- 0.05
-0.550	1.82 +- 0.09	-0.22 +- 0.13	-0.46 +- 0.05
-0.450	2.07 +- 0.09	-0.43 +- 0.16	-0.53 +- 0.06
-0.350	2.33 +- 0.11	0.00 +- 0.23	-0.50 +- 0.09
-0.250	2.68 +- 0.15	-0.10 +- 0.34	-0.40 +- 0.13
-0.150	2.90 +- 0.25	-0.11 +- 0.51	-0.45 +- 0.19
-0.050	2.67 +- 0.40	-0.31 +- 0.71	-0.27 +- 0.28
	W = 1.505 GeV	ϵ = 0.91	q^2 = 0.60 GeV^2
-0.985	0.47 +- 0.07		
-0.935	0.80 +- 0.06	0.06 +- 0.11	-0.24 +- 0.05
-0.850	1.03 +- 0.13	-0.04 +- 0.21	-0.33 +- 0.09
-0.750	1.24 +- 0.19	-0.06 +- 0.26	-0.28 +- 0.19
-0.650	1.62 +- 0.09	-0.17 +- 0.11	-0.45 +- 0.06
-0.550	1.92 +- 0.09	-0.26 +- 0.14	-0.55 +- 0.06
-0.450	2.17 +- 0.11	-0.46 +- 0.21	-0.45 +- 0.09
-0.350	2.52 +- 0.14	-0.48 +- 0.27	-0.56 +- 0.12
-0.250	2.42 +- 0.17	-1.19 +- 0.39	0.00 +- 0.15
	W = 1.535 GeV	ϵ = 0.90	q^2 = 0.59 GeV^2
-0.985	0.53 +- 0.08		
-0.935	0.85 +- 0.08	-0.02 +- 0.12	-0.18 +- 0.07
-0.850	0.89 +- 0.07	-0.18 +- 0.11	-0.14 +- 0.06
-0.750	1.15 +- 0.10	-0.31 +- 0.18	-0.26 +- 0.11
-0.650	1.58 +- 0.19	0.14 +- 0.28	-0.20 +- 0.18
-0.550	1.63 +- 0.09	-0.54 +- 0.16	-0.27 +- 0.07
-0.450	1.88 +- 0.11	-0.28 +- 0.24	-0.26 +- 0.11
-0.350	1.73 +- 0.14	0.16 +- 0.27	-0.21 +- 0.13
-0.250	2.43 +- 0.32	-0.57 +- 0.50	-0.24 +- 0.27
	W = 1.565 GeV	ϵ = 0.90	q^2 = 0.58 GeV^2
-0.985	0.43 +- 0.07		
-0.935	0.61 +- 0.12	-0.36 +- 0.20	0.11 +- 0.10
-0.850	0.81 +- 0.05	-0.19 +- 0.08	-0.06 +- 0.04
-0.750	0.86 +- 0.08	-0.37 +- 0.16	-0.23 +- 0.08
-0.650	1.36 +- 0.17	0.22 +- 0.31	0.04 +- 0.14
-0.550	1.25 +- 0.08	-0.24 +- 0.18	-0.15 +- 0.08
-0.450	1.26 +- 0.11	-0.49 +- 0.29	0.09 +- 0.13
	W = 1.595 GeV	ϵ = 0.89	q^2 = 0.57 GeV^2
-0.985	0.38 +- 0.11		
-0.850	0.88 +- 0.08	-0.26 +- 0.14	0.03 +- 0.06
-0.750	1.35 +- 0.15	0.24 +- 0.26	0.35 +- 0.13

The measured angular distributions range from forward to backward production angles in some cases. The polarization terms $\sigma_U + \epsilon\sigma_L$, σ_P and σ_I have been determined by least squares fits of the differential cross sections at fixed W, q^2 and $\cos\theta^*$

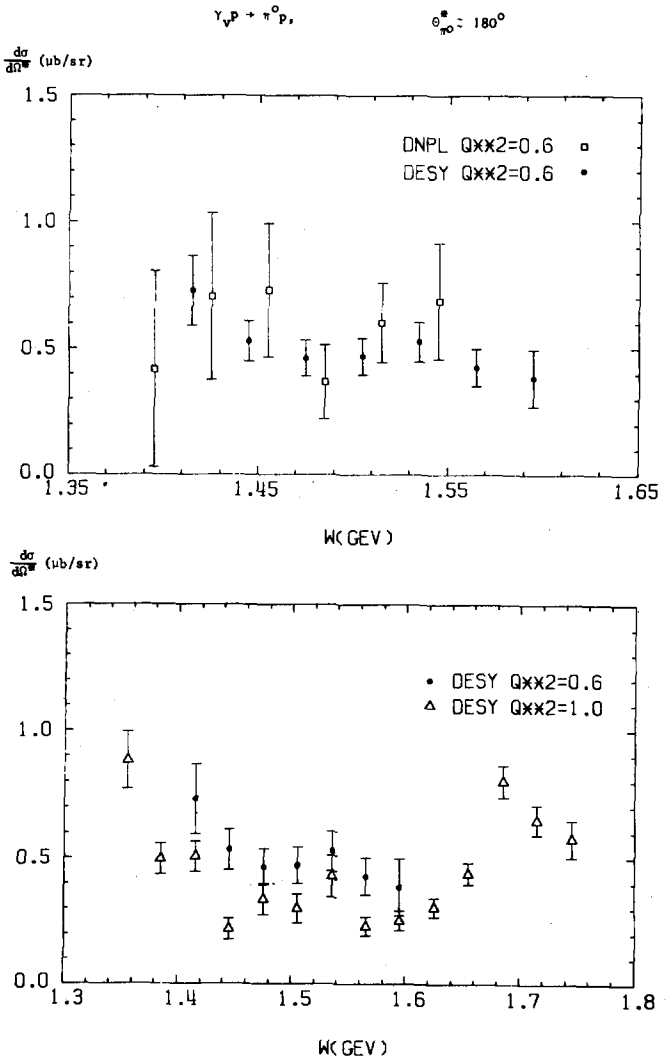

Fig. 3. Backward π^0 production cross sections as a function of W at $q^2 = 0.6$ GeV^2 from DNPL [3] and at $q^2 = 0.6$ and 1 GeV^2 from this experiment.

according to the ϕ dependence of eq. (2). Results of these fits are given in figs. 6 to 8 and table 1 only if a range in ϕ of at least 100° is covered. This is the case essentially in the backward hemisphere. The backward cross sections $\sigma_U + \epsilon\sigma_L$ (fig. 3) have been obtained by averaging over all events of a given W, q^2 bin with $\cos\theta^* < -0.97$.

We estimated the total cross section σ_{tot} of $\gamma_v p \to \pi^0 p$ in some range of W, where

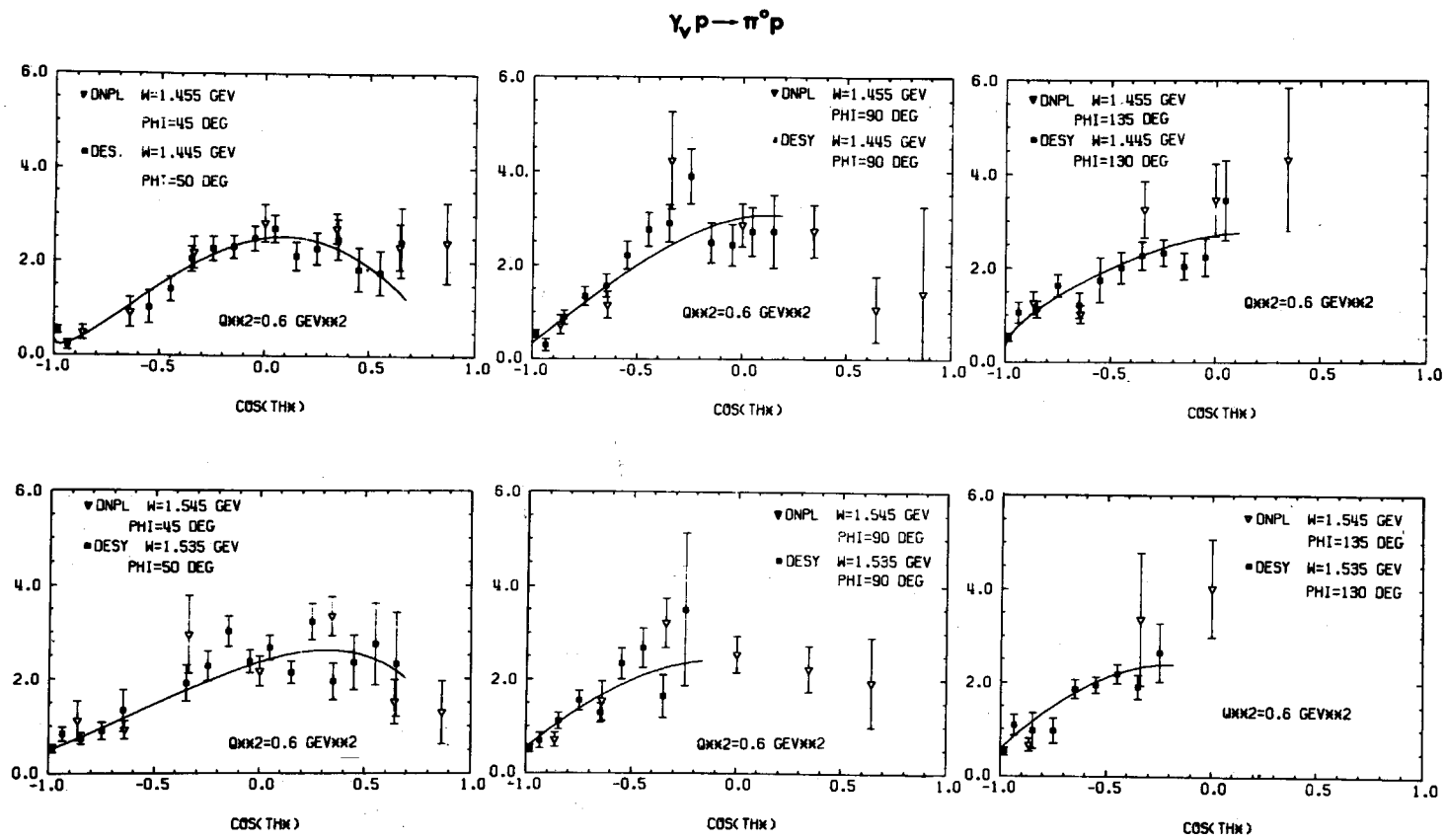

Fig. 4. Examples of angular distributions at $q^2 = 0.6$ GeV^2 in comparison with data from DNPL [3]. Solid line: cross section computed from the angular coefficients (see text).

the angular coverage was sufficient. σ_{tot} was computed according to eq. (4) from the angular coefficients which were determined by least squares fits to all differential cross sections of a given W, q^2 bin. For $W \leqslant 1.565$ GeV eq. (3) has been used. For larger W values the coefficients A_4, C_2 and D_3 have been included. The curves in figs. 4 to 7 represent the cross sections according to these fits. The results on σ_{tot} are given in table 2 and in fig. 9 together with the results [9] of a previous ex-

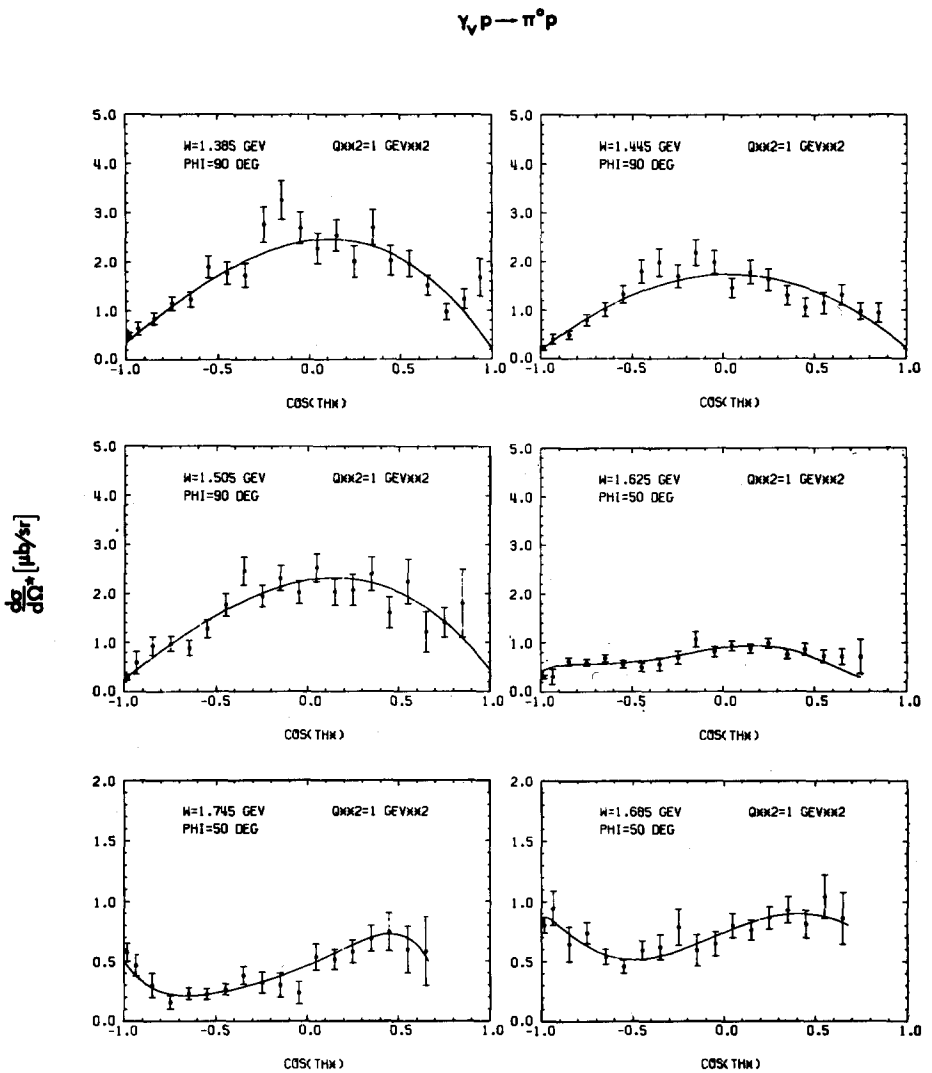

Fig. 5. Examples of angular distributions at $q^2 = 1$ GeV^2. Solid line: cross section computed from the angular coefficients (see text).

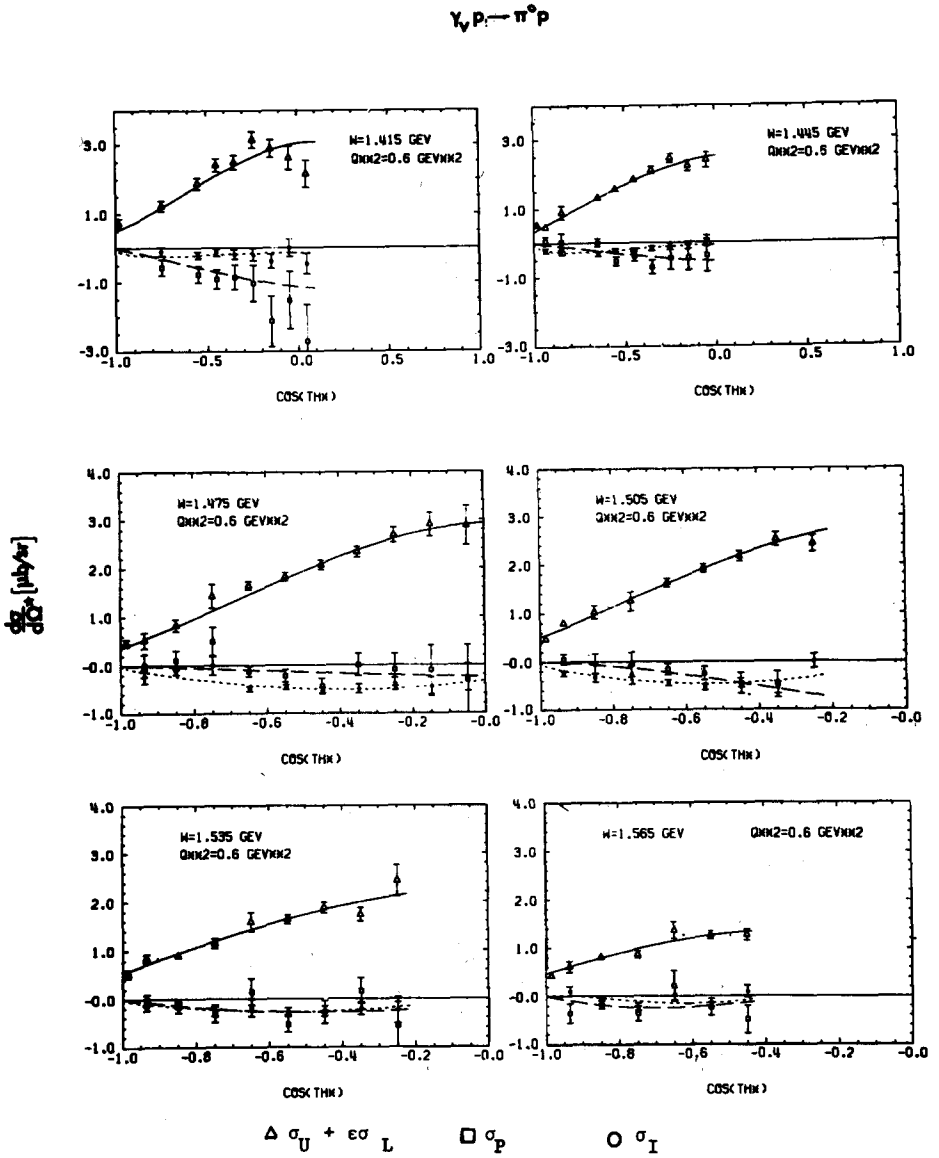

Fig. 6. Angular distributions of $\sigma_U + \sigma\epsilon_L$ (Δ), σ_P(□) and σ_I (o) at $q^2 = 0.6$ GeV^2. Curves: $\sigma_U + \epsilon\sigma_L$ (–), σ_P (– –), and σ_I (– – ––) as computed from the angular coefficients (see text).

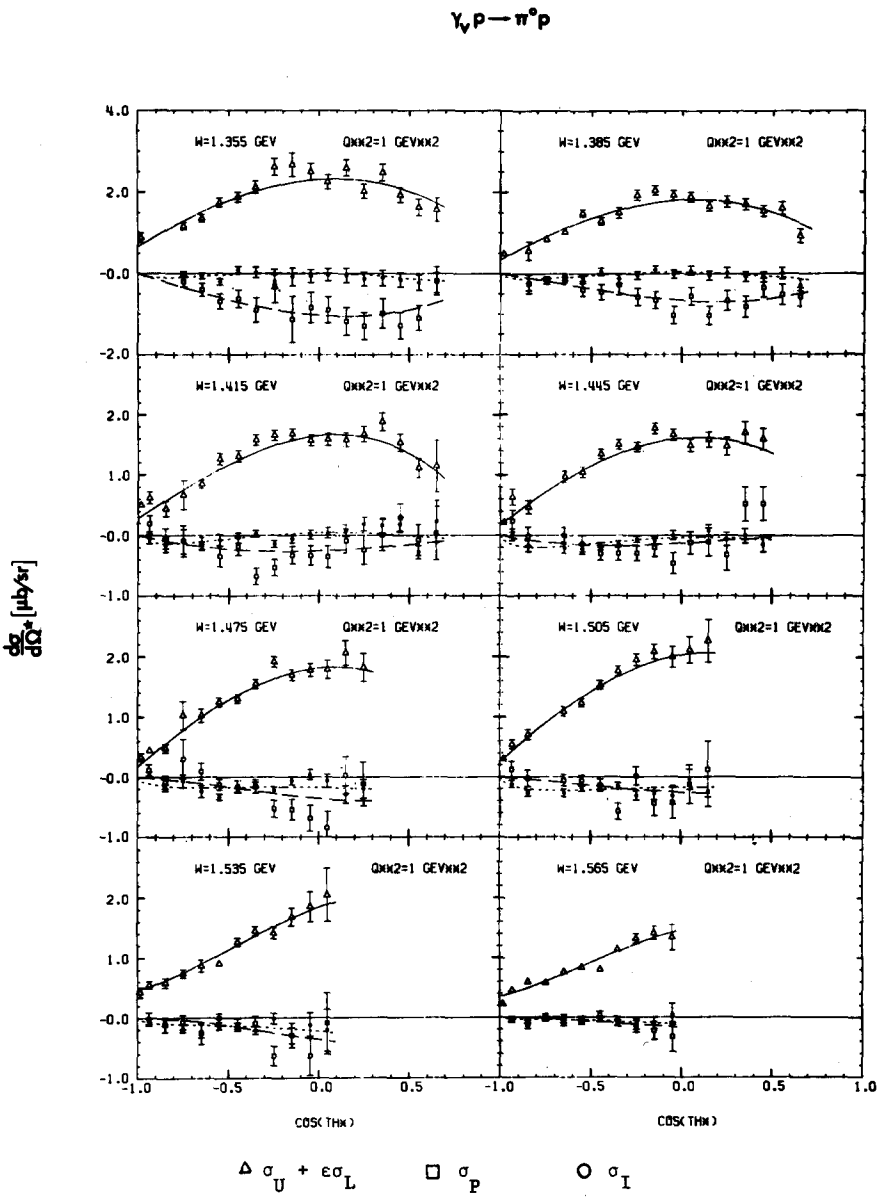

Fig. 7a. Angular distributions of $\sigma_U + \epsilon\sigma_L$ (Δ), σ_P (□), and σ_I (○) at $q^2 = 1$ GeV^2 in the W range 1.355 GeV to 1.565 GeV. Curves: $\sigma_U + \epsilon\sigma_L$ (–), σ_P (– –), and σ_I (- - - -) as computed from the angular coefficients (see text).

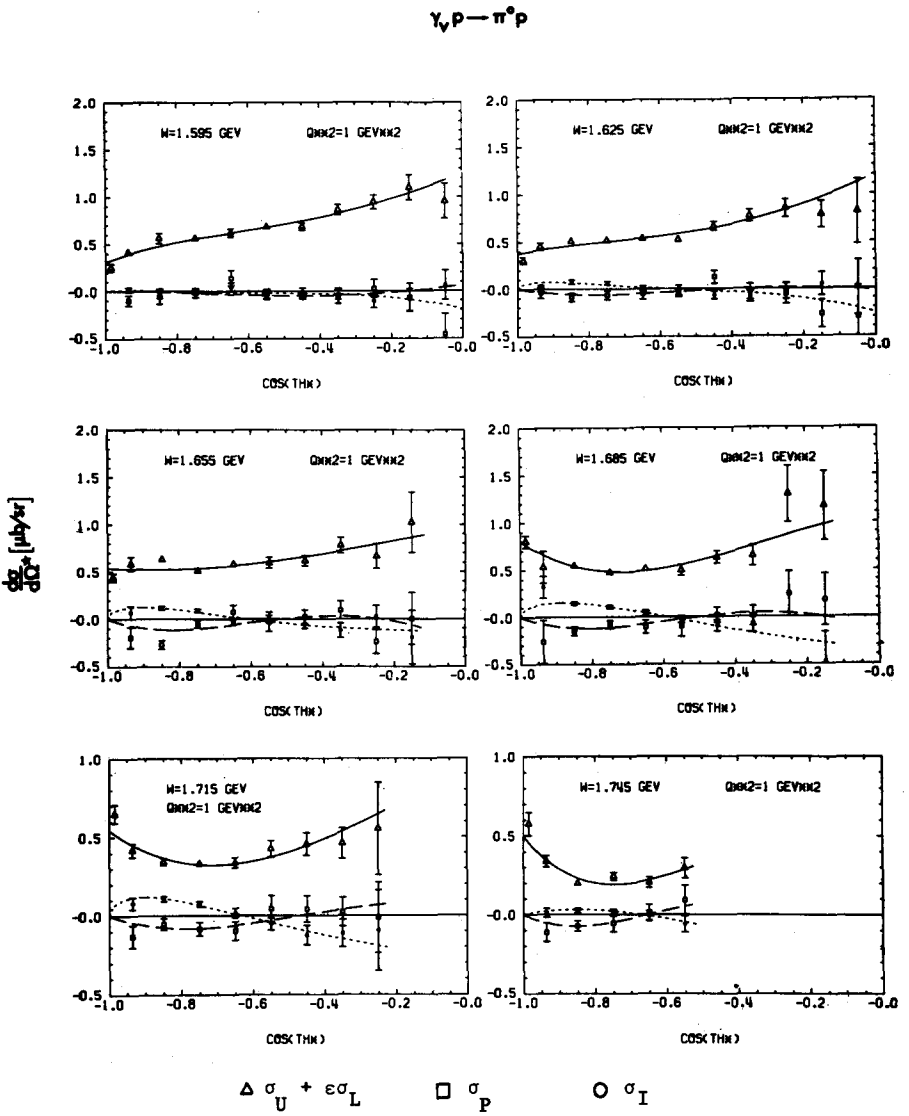

Fig. 7b. Same as fig. 7a in the W range 1.595 GeV to 1.745 GeV.

Table 2
Estimates of σ_{tot} of $\gamma_v p \to \pi^0 p$ from the fitted angular coefficients (see text).

W [GeV]	σ_{tot}[μb] $q^2 \approx 1$ GeV^2	σ_{tot} [μb] $q^2 \approx 0.6$ GeV^2
1.325	30.9 ± 2.7	
1.355	22.2 ± 0.6	
1.385	16.4 ± 0.4	
1.415	14.2 ± 0.4	22.5 ± 4.1
1.445	14.3 ± 0.4	21.0 ± 2.9
1.475	15.8 ± 0.6	18.2 ± 4.3
1.505	18.4 ± 1.0	16.4 ± 4.9
1.535	18.2 ± 1.5	18.6 ± 7.0
1.565	13.2 ± 1.5	
1.595	15.0 ± 3.4	
1.625	16.6 ± 4.1	
1.655	10.5 ± 5.1	
1.685	10.1 ± 6.6	
1.715	13.9 ± 7.4	

The errors are statistical only (ϵ, q^2 as in table 1).

periment [6]. Due to lack of acceptance at small θ^* there may be considerable errors at $q^2 = 0.6$ GeV^2 and at $W \gtrsim 1.6$ GeV at $q^2 = 1$ GeV^2. Total $\gamma_v p \to X$ cross sections are shown for comparison.

We have compared our results with the data of Shuttleworth et al. [3] and Driver et al. [4]. In general we find that our differential cross sections are consistent with both experiments. A comparison with the Daresbury data [3] is shown in figs. 3 and 4. Our results on total cross sections at $q^2 = 0.6$ GeV^2 (table 2) are below these from ref. [3] by about 25%, which is of the order of uncertainties to be expected due to the lack of acceptance mentioned above. A complete list of all measured differential cross sections will be given elsewhere.

The backward cross sections (fig. 3) show considerable structure in the third resonance region indicating the presence of resonant amplitudes of total helicity $\frac{1}{2}$ of the ingoing virtual photon and proton. In the second resonance region helicity $\frac{3}{2}$ excitation seems to be more important than helicity $\frac{1}{2}$ excitation: at W about 1.5 GeV the backward cross sections are very small and show no significant resonance structure (fig. 3) and the angular distributions (figs. 4 to 7) are similar to those observed in photoproduction. It is one of the results of the multipole analysis of Devenish and Lyth [5], that helicity $\frac{1}{2}$ excitation increases in relative importance as q^2 changes from zero to a few GeV^2. Moreover this increase seems to occur more rapidly at $F_{15}(1688)$ than at $D_{13}(1525)$. In this analysis [5] some preliminary differential cross sections of the present experiment with ϕ close to 90° had been used.

As shown in a recent experiment [10] the angular distribution of the reaction

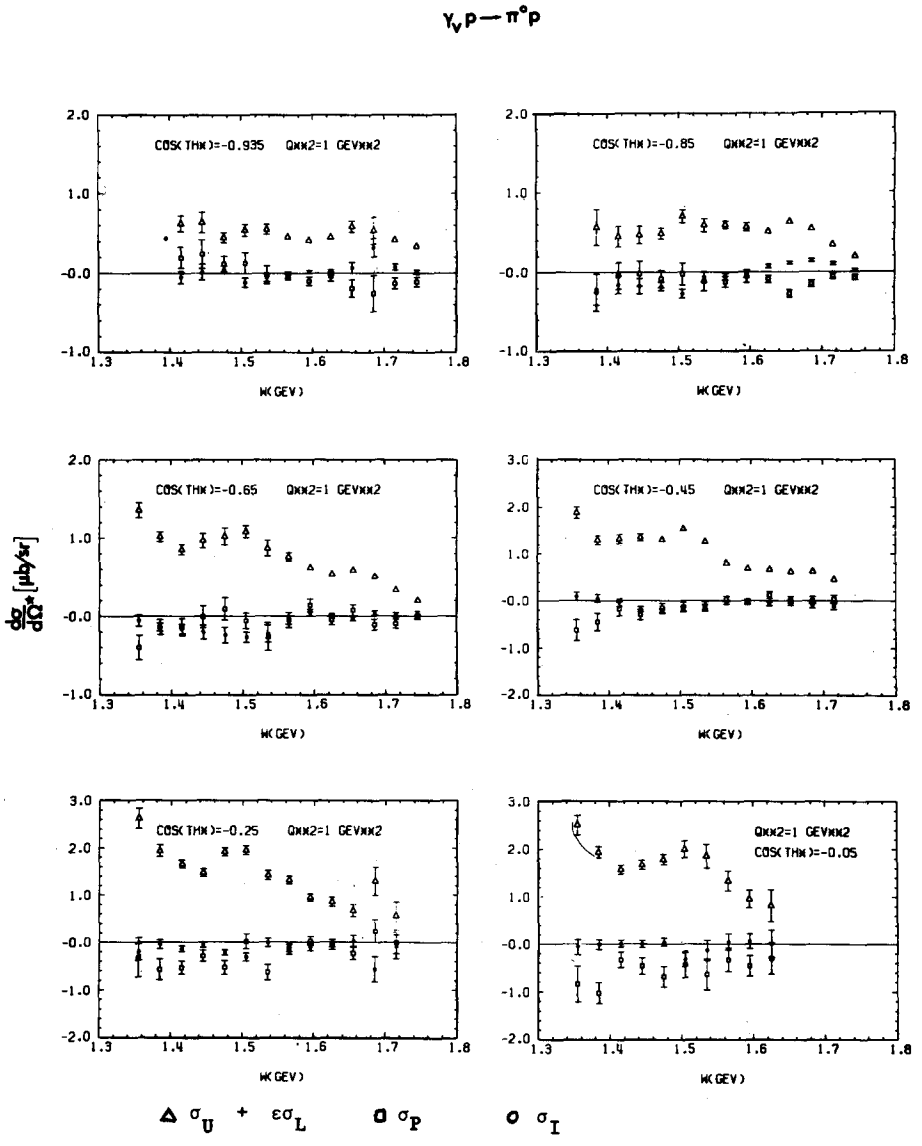

Fig. 8. $\sigma_U + \epsilon\sigma_L$ (▽), σ_P (□) and σ_I (○) as a function of W at different values of $\cos\theta^*$ at $q^2 = 1$ GeV^2.

$ep \to ep\pi^0$ at $W \approx 2.55$ GeV changes rapidly going from photoproduction to space-like four momentum transfers. It was remarked by Moorhouse [11] that this change may be foreshadowed in the region of $F_{15}(1688)$ just as the dip at $t \approx -0.5$ GeV^2 and the subsequent hump first appears in this region in photoproduction.

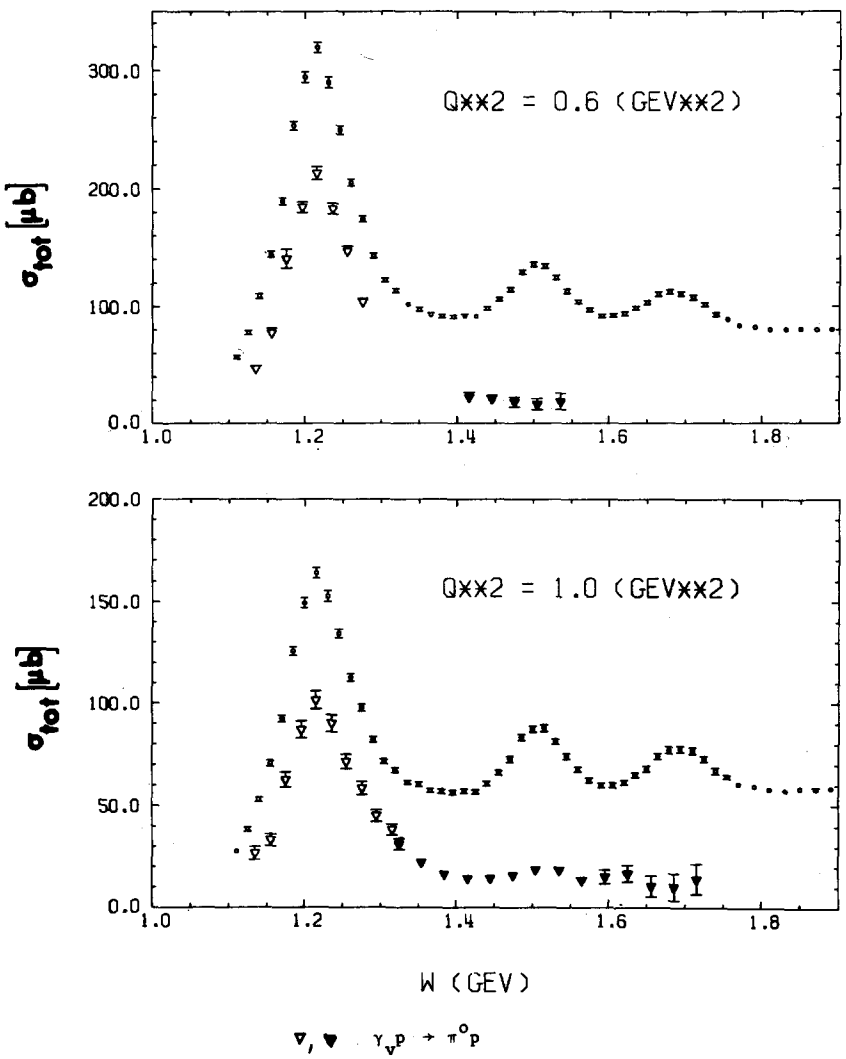

Fig. 9. Total cross section of $\gamma_v p \to \pi^0 p$ (▽ from ref. [9], ▼ this experiment) in comparison to the total cross section of $\gamma_v p \to X$ (o from ref. [12]).

The present data cover the range from $t \approx -0.5$ GeV^2 up to the backward direction at $W \gtrsim 1.688$ GeV. It is interesting to note that the cross section at $q^2 = 1$ GeV^2 (fig. 5) essentially decreases from $t = -0.5$ GeV^2 ($\cos\theta^* \approx 0.65$) to $t = -1.4$ GeV^2 ($\cos\theta^* \approx -0.15$) or even up to $t \approx -2$ GeV^2 ($\cos\theta^* \approx -0.65$) without the strong rise observed at $q^2 = 0$ at $|t| \geqslant 0.5$ GeV^2.

We gratefully acknowledge the excellent performance of the Synchrotron crew, the Hallendienst and the Rechenzentrum. We thank J. Koll, G. Singer, K. Thiele, H. Weiss and Mrs. K. Schmoger for careful technical work, E. Ganssauge for his help in the early stage of the experiment.

References

[1] J.-C. Alder, F.W. Brasse, W. Fehrenbach, J. Gayler, R. Haidan, G. Glöe, S.P. Goel, V. Korbel, W. Krechlok, J. May, M. Merkwitz, R. Schmitz and W. Wagner, Nucl. Phys. B91 (1975) 386.
[2] J.-C. Alder et al., Nucl. Phys. B99 (1975) 1.
[3] W.J. Shuttleworth, A. Sofair, R. Siddle, B. Dickinson, M. Ibbotson, R. Lawson, H.E. Montgomery, R.D. Hellings, J. Allison, A.B. Clegg, F. Foster, G. Hughes and P.S. Kummer, Nucl. Phys. B45 (1972) 428.
[4] C. Driver, K. Heinloth, K. Höhne, G. Hofmann, P. Karow, D. Schmidt, G. Specht and J. Rathie, Nucl. Phys. B33 (1971) 84.
[5] R.C.E. Devenish and D.H. Lyth, Nucl. Phys. B93 (1975) 109.
[6] J.-C. Alder et al., Nucl. Phys. B46 (1972) 573.
[7] K. Berkelman, Proc. Int. Symp. on electron and photon interactions at high energies, Hamburg, 1965;
M. Gourdin, Nuovo Cimento 21 (1961) 1094.
[8] G. Miller, Thesis, Stanford University (1971).
[9] J. Gayler, Thesis, DESY F21-71/2 (1971);
J. May, Thesis, DESY F21-71/3 (1971).
[10] F.W. Brasse, W. Fehrenbach, W. Flauger, J. Gayler, S.P. Goel, R. Haidan, U. Kotz, V. Korbel, D. Kreinick, J. Ludwig, J. May, M. Merkwitz, K.-H. Mess, P. Schmüsser and B.H. Wiik, DESY 75/23 (1975).
[11] R.G. Moorhouse, Rapporteur's talk presented at the Palermo Conf., June 1975.
[12] F.W. Brasse, W. Flauger, J. Gayler, S.P. Goel, R. Haidan, M. Merkwitz and H. Wriedt, DESY preprint, to appear.